

DYNAMIC CALIBRATION OF TORQUE TRANSDUCERS APPLYING ANGULAR ACCELERATION PULSES

Rafael S. Oliveira¹, Renato R. Machado¹, H. Lepikson², Thomas Fröhlich³, René Theska³

¹Instituto Nacional de Metrologia, Qualidade e Tecnologia - INMETRO, Duque de Caxias, Brazil
rsoliveira@inmetro.gov.br

²Federação das Indústrias do Estado da Bahia - FIEB, Salvador, Brazil

³Ilmenau University of Technology - TU-ILMENAU, Ilmenau-TH, Germany

Abstract: The traceability of the torque quantity finds a gap when there is a regime with torque variation rates, once the traditional calibration methods define the references to be of null torque variation (static) or of very low torque rate (continuous). This paper presents a method for providing torque traceability to rotating sensors under higher torque variation rates. The principle of applying acceleration pulses to rotating shafts with mounted reference mass moments of inertia is presented and then followed by the description of sequential proceedings for obtaining the analysis in the time domain. Demonstrative experimental data is used in order to give a qualitative approach to the theoretical description of these methods involved.

Keywords: Dynamic torque, Torque metrology, High torque variation rate, Torque transducer, Angular acceleration.

1. INTRODUCTION

The current traceability for torque transducers used in all applications is based on static proceedings and static standard systems. The traditional calibration standards and guidelines, such as [1], define the reference value as a completely static one, preferably using a dead weight and lever-arm torque generation machine, coming along with a large period of stabilization during the load sequences.

However, in regimes where it is important to have the measurement of torque during periods with high torque rates, there must be a demand for different patterns. In addition, most of these applications also use sensors under rotation conditions, what is also totally not approached in the traditional standard. Traceability alternatives must be found out in order to cover these non-static measurement systems.

The research for new methods of providing traceability to the torque quantity is growing [2-4] and the dynamic approach is also getting into focus. This paper advances in the presentation of a contribution for this research field and how this proposal, first introduced in [5-7] and now reviewed in its main proceedings, fits in the dynamic metrology scenario, once there are different interpretations for the definitions or statements on how dynamic can measurements be.

1.1. THE DYNAMICS OF THE PROPOSAL

To understand the dynamic basics of the proposal, it is important to point out two main facts that delineate the extremes where it fits within.

First approaches to the traceability of dynamic torque were presented in [8, 9], where an oscillatory (sinusoidal) regime was applied to the measurement system through a frequency range sweep, followed by the frequency domain analysis of data. This method evaluates both amplitude and phase responses of the device under calibration

On the other hand, [1] presents the continuous calibration method as an alternative to the static one, which can reduce the total calibration time in 1/10. However, beyond the necessity of the equipment to be able to detect fast readings, instead of stabilized ones, rapid changes in torque values cause unwanted effects on transducer behaviour such as creep phenomena and high reversibility errors [10]. A critical torque rate of around $17 \text{ N}\cdot\text{m}\cdot\text{s}^{-1}$, during incremental loading, is found in [11] where the linearity deviation results are very disturbed. In [12] it is shown that the different digital filtering parameters and the rates of torque application influence directly on the stability of the readings. These behaviours were attributed to dynamic effects and then could not be followed by a simple continuous *quasi-static* loading methodology.

So, within these two marks, one question remains: How to cover traceability for loading torque profiles, with high rates of variation of the quantity and keeping direct analysis to the time domain?

The research presented in this paper keeps the analysis in the time domain, being interpreted and summarized as a next step on the generation of reference torque pulses (no oscillations) with high torque rates, together with the sensor's rotation regimes, when the continuous torque calibration proceeding turns insufficient.

2. CALIBRATION METHOD DESCRIPTION

As already introduced in [2], the method proposed is based on the principle of applying reference dynamic torque (T) to the transducer through the acceleration ($\dot{\omega}$) of a part with a known mass moment of inertia - $\text{MMI}(\theta)$ as summed in equation 1.

$$T = \theta \cdot \dot{\omega} \quad (1)$$

In a rotating shaft, the dynamic regime proposed corresponds to the acceleration pulse period between two angular speed steps. With the speed signal measured, acceleration data can be reached through its differentiation.

It is important to highlight that the startups are done with the whole system under rotation. Therefore, there are the ramps between speed steps, where the reference acceleration is extracted, and then the speed is returned for the previous step through a braking period. Figure 1.a shows an example of this regime in time, with a system composed by an electric motor, an encoder and a torque transducer coupled to it (*configuration I* in Figure 2), running three consecutive acceleration ramps between speed steps.

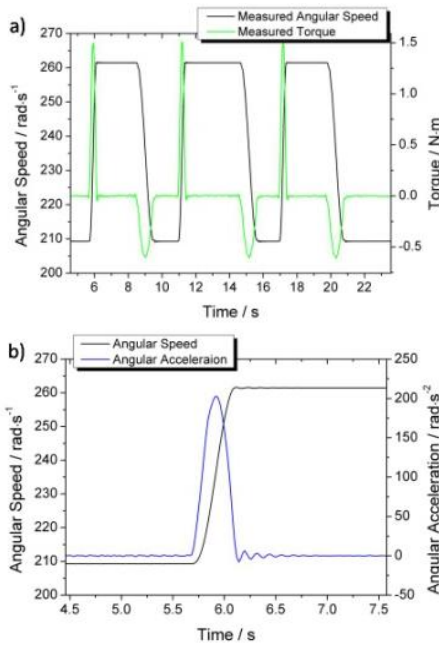


Figure 1. (a) Angular speed steps; (b) Corresponding acceleration ramp.

Figure 1.b shows a zoom in the time axis, with the measured speed signal and the calculated acceleration pulse during the speed step period. This period of acceleration pulse correspond to the possibility of applying high torque rates, and the development of strategies for reaching the torque traceability during this regime is the challenge proposed by this research.

In a broad approach, the proposed method should:

1. Identify a time dependency of the quantity;
2. Prioritize the application of torque rates;
3. Evaluate the differences between the values read in the transducer (calibration curves) and those generated in the reference;
4. Evaluate the susceptibility to different kinematic conditions;
5. Occur throughout the range of application of torque;
6. Assess reproducibility in sequential loadings.

2.1. SEQUENCE OF OPERATION

A sequence of operation is proposed in order to get a logical path to reach the intended torque profile and the range of stimulations necessary to better evaluate the sensor under different kinematic conditions. Figure 2 shows the proposed mechanical system including the driver (electric motor), the transducer, the encoder and the inertial shaft.

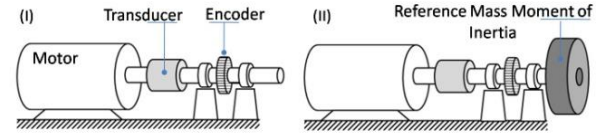


Figure 2. Assembly with the sensor in line with different configurations of inertia.

The *Configuration I* shows the initial assembly with the main, and constants, components of inertia in the shaft, which will be called the initial mass moment of inertia (θ_i). The inertial torque (T_{ii}) generated by these components under acceleration will correspond to the measured torque (T_{ti}) in the transducer. This value will be considered a tare value for the evaluation of the net measured torque.

In the sequence of measurements and startups, *Configuration II* shows the inclusion of a reference mass moment of inertia (θ_r) to the main shaft. Now the assembly's total inertia will generate an inertial torque of ($T_{ii} + T_{ir}$) and that will correspond to a measured torque of (T_t). The net measured torque (T_{ti}) will be the difference between values measured in both configurations and corresponds to the evaluable inertial reference torque (T_{ir}). These correspondences between inertial configurations and torques can be found on Table 1.

Table 1. Correspondence between parameters and assembly Configurations I and II of Figure 2.

	<i>Config. I</i>	<i>Config. II</i>
MMI of the shaft	θ_i	$\theta_i + \theta_r$
Generated inertial torque	T_{ii}	$T_{ii} + T_{ir}$
Gross measured torque	T_{ti}	T_t
Net measured torque ($T_{ti} - T_t$)		T_{ir}

Figure 3 shows the sequence of operation of this system to get sequential loadings varying the conditions of inertia and accelerations possible to be applied to a certain assembly of motor, shaft and transducer. From this sequence, we can see that, once an inertial condition is set, sequential speed steps and accelerations will be applied to that configuration (*loops 1 and 2*). After that, the inertial configuration is changed (*loop 3*) and the same sequence of acceleration and speeds must be applied. Therefore, after that, measured data of speed and torque are evaluated to find the corresponding dynamic situations and net values can be calculated.

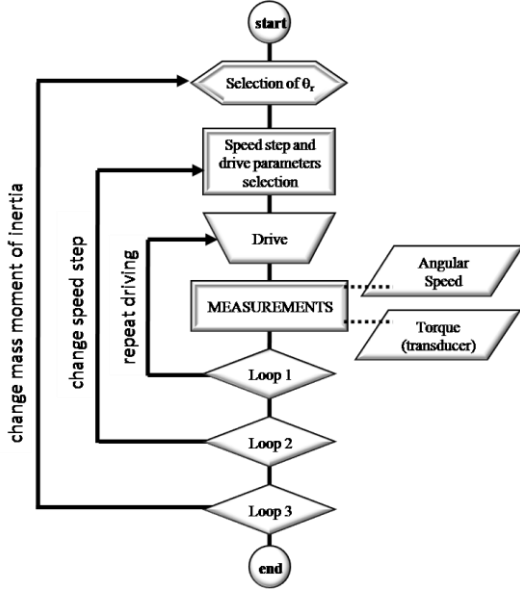


Figure 3. Sequence of operation to test different inputs to the sensor

2.2.METHODS OF ANALYSIS

Two methods of analysis are proposed based on the relation between the quantities involved. Both are applied from the same pack of measured data using only offline signal processing, including the calculation of the acceleration data from the differentiation of the speed data.

To help elucidating the proposed comparison methods, we will use, in a qualitative purpose, a couple of real data, obtained from a pack of experiments carried out during the research, together with the method explanation and some comments. The experimental assembly (Figure 4) was quite similar to that described in Figure 2, except for the fact that the encoder used for speed measurement was the slot type encoder included in the T12 torque transducer from HBM. Results for the driving of two inertial discs, named #D20 and #D40, under one acceleration profile are used here.



Figure 4. Experimental assembly for testing runs in the measuring shaft with initial configuration (left) and with #D40 (right).

The first method is called "direct calibration" and uses equation 2.a, expanded in 2.b, to evaluate the error results (E), comparing the average values of reference torque (\bar{T}_{ir}) to the measured net torque value at the transducer (\bar{T}_{tl}), both synchronized and indexed in time intervals as i .

$$E_{(i)} = \bar{T}_{tl(i)} - \bar{T}_{ir(i)} \quad (2.a)$$

$$E_{(i)} = (\bar{T}_{t(i)} - \bar{T}_{ti(i)}) - (\bar{\omega}_{(i)} \cdot \theta_r) \quad (2.b)$$

Figure 5 shows the \bar{T}_{tl} and \bar{T}_{ir} curves, for each inertial configuration with discs, obtained from the averages of these parameters acquired in the runs inside therepetitions of 'loop 1' applied to the system and the corresponding results of E . Both inertial configurations were started under the same speed step and same acceleration profile, so they use the same averaged tare torque value.

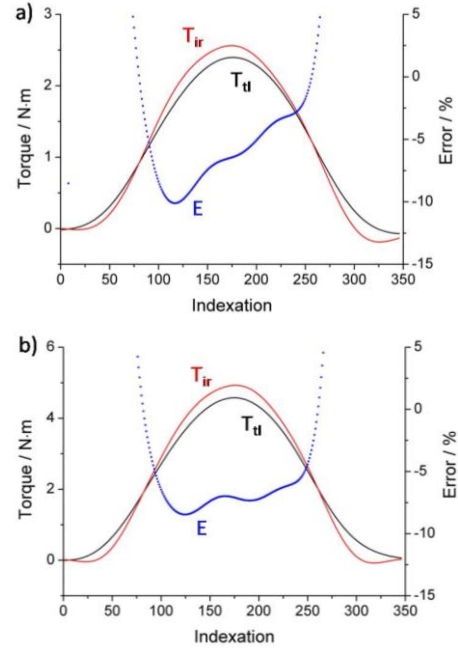


Figure 5. Error result according to the method of 'direct calibration' in the inertial configurations of (a) #D20 and (b) #D40.

From these graphical results it can be noted that there is a time dependency and also a tendency to the error plots, even if different for the inertial configurations. The error for the loading side (left side) of the curve is less than the error for the unloading side (right side).

Due to the instability in the extremes of the pulse curves, where acceleration and inertial torque are around zero value, what can be better noted in the acceleration curve of Figure 1.b, it will cause a huge instability to the error analysis. This induces the methodology to require a limitation for the studied range of torque within each comparison proceeding corresponding to a pair of inertia and acceleration start-up parameters.

The second method is called "indirect calibration" and intends to be a more simple process, with the analysis based on the linearity of the proposed principle and the differences between angular slopes of linear fitting curves.

It deals with the theoretical linear relationship between the reference acceleration and the torque value measured from the transducer. In order to get it simple, data of T_t and $\dot{\omega}$ can be put together and a linear fitting curve can be calculated, where now there is a new parameter called 'adjusted torque' ($T_{adj,t}$), which will be expressed in terms of $\dot{\omega}$ (equation 3) and pass through the origin (0,0). This

method does not demand for synchronization of torque readings.

$$T_{adj,t} = \alpha \cdot \dot{\omega} \quad (3)$$

The angular coefficients (α) of these expressions will be calculated as one for each inertial configuration under the same acceleration profile, including the initial configuration, also working here as a tare reference. Figure 6 shows the graphical interpretation of the method, calculating the slopes for the two inertial configurations, $\theta_{s_#D20}$ and $\theta_{s_#D40}$, of the shaft.

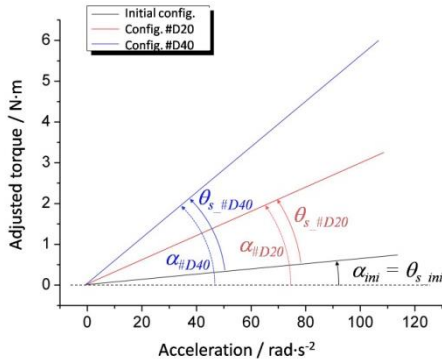


Figure 6. Graphical demonstration of the evaluable angular coefficients (slopes).

Figure 6 shows the graphical interpretation of equation 3, calculating the slopes for the two inertial configurations of the shaft. Once the slopes are calculated, they can be compared to the MMI of reference, resulting in another error parameter (E_θ), as shown in equation 4.

$$E_\theta = \theta_s - \theta_r \quad (4)$$

Another interesting parameter that can be measured based on this method is the linearity deviation between $T_{adj,t}$ values (red line) and the measured T_t values (grey dots), as shown in figure 7. This gives another idea of the behaviour of the sensor referring to the physical principle proposed.

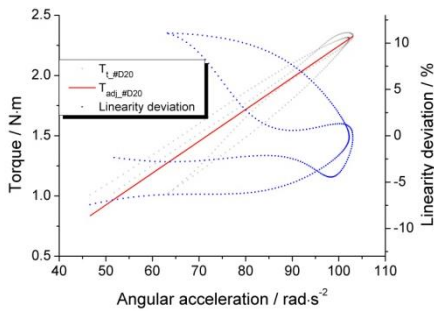


Figure 7. Linearity deviation for the configuration of #D20.

From this graph, representing two runs for #D20, it is possible to observe that there is a better convergence (linearity deviation surrounding zero value) on the upper part of the line, above 1.5 N·m, corresponding to the top of the pulse torque load curve. This refers to the necessity of determining a cut point in the torque domain (T_{cp}), restricting the analysis to a more stabilized region on the load regime.

In the same way that happened to the direct calibration error, this fact would also influence the evaluation of error and Table 2 shows different values of relative E_θ for both inertial configurations with different torque cut points T_{CP} .

Table 2. Evaluated error E_θ for different.

Inertial config.	T_{CP} / N·m	θ_s / kg·m ²	θ_r / kg·m ²	E_θ
#D20	2.0	0.02355	0.02489	5.4%
	1.5	0.02275		8.6%
#D40	4.0	0.04650	0.04957	6.2%
	3.5	0.04571		7.8%

There it can be noted that, the closer the T_{CP} is from the top, better error results it will get, but narrower will be the range analyzed.

2.3. HIGHLIGHTS FOR UNCERTAINTY

A first approach to the evaluation of the uncertainty of measurement was presented in [2], with the identification of the basic components and their quantitative estimative. However, the development of the research demanded for the increment and detailing of those components. In the direct calibration method for example, Figure 8 shows a good resume of these developed components of uncertainty for the construction of U_E , mainly divided into the uncertainty for the measured torque $U_{T_{tl}}$ and the uncertainty of the reference inertial torque axis $U_{T_{ir}}$.

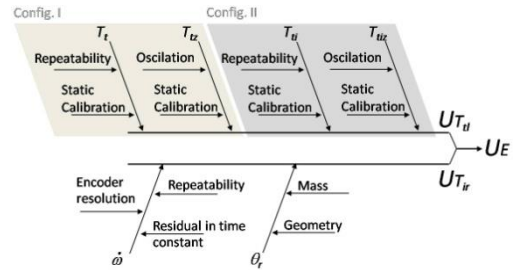


Figure 8. Main uncertainty contributions for U_E .

From that diagram we can highlight that for the measured torque side, there will be contributions from both inertial configurations I and II. Within each configuration, there are the repeatability of the curves during *loop 1* and after synchronization, the oscillation of initial zero levels (see Figure 9) and the static calibration uncertainty for the analyzed point/range. This last contribution is important because there is the link between the static results and the dynamic ones.

For the inertial torque side, there are the uncertainty contributions on mass moment of inertia and acceleration. The MMI's contributions are related to the measurement of mass and geometry. The acceleration has the contributions of the constancy of the time intervals in the speed signal differentiation process, parameter directly related to the acquisition system, the influence of the encoder resolution or static calibration, once there is no system for the

calibration of speed and the repeatability of the acceleration curves during the loops.

For the indirect calibration method, the main contributions of uncertainty will be about the method for calculating the linear fitting curve.

2.4. HOW TO REPORT THE RESULTS

The dynamic calibration proposal included two different methods of analysis, what can be interesting to be joint in a same test report. Nevertheless, the report should contain all the parameters of interest, due to the vast possibility of combinations, such as the following suggestions:

- Characterize the interesting torque pulses (peak torque, maximum torque rate, acceleration or deceleration, clockwise or anticlockwise);
- Highlight the static uncertainties;
- Report kinematic conditions: speed step, acceleration times and reference MMI's used;
- Report E and its uncertainty U_E in the graphic mode or select the most interesting points in the load curve and do it individually, in a table. Figure 9 shows the torque load curve for the experiment with the #D20 inertia configuration as an example. In the graph, there is the average \bar{T}_{tl} and the confidence interval for the uncertainty U_E .
- Report E_θ together with the corresponding T_{cp} , such as in Table 2.

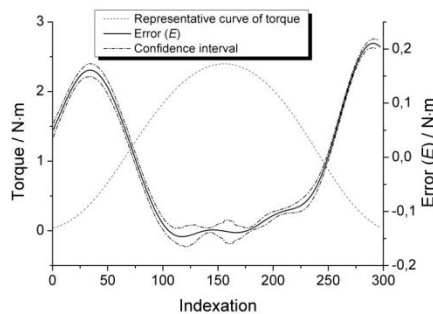


Figure 9. Torque load curve with the Error and the respective uncertainty interval envelop.

3. DISCUSSION

The paper gives focus to the needs of better evaluating, in the time domain, those regimes of torque with the variation of the quantity.

With these experiments, the physical principle was validated. Figure 10 shows the torque curves, obtained from the averages for the measurements carried out during the loops with both inertial configurations and the same tare curve. The green box identifies the initial zero level and there is an oscillation around this considered zero value, after individual tare proceeding of each curve. Figure 11 shows the achieved torque rate at these configurations, which are calculated as the first differentiation of the net torque curves.

These maximum rates of torque reached at the experiments were $\pm 10 \text{ N}\cdot\text{m}\cdot\text{s}^{-1}$ and $\pm 15 \text{ N}\cdot\text{m}\cdot\text{s}^{-1}$ for the

#D20 and #D40 inertial configurations respectively, as can be seen in Figure 9.

The capacity of a system to reach high torque rates will depend on the capacity of the electric motor to accelerate the shaft within its limits of maximum acceleration torque. The system used for the experiments on this research was an adaptation of an electric motor test bench at CEPEL¹ to support the shafts, bearings and the inertial discs. Then, the laboratory kept some secure and safe configurations that limited the acceleration levels of the motor.

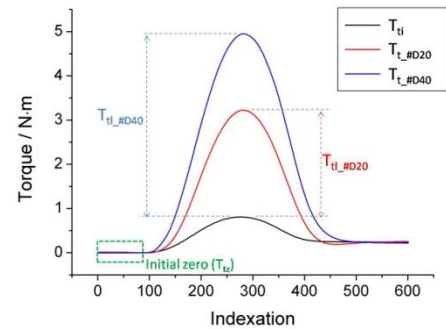


Figure 10. Synchronized (indexed intervals) torque curves.

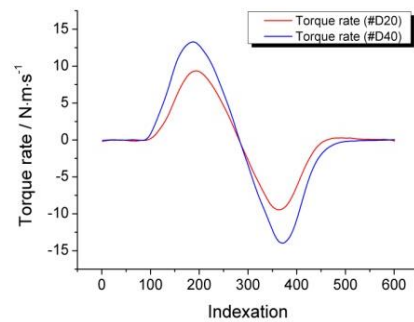


Figure 11. Torque rate curves for both inertial configurations.

The direct calibration method showed the temporal dependency of errors and the indirect method evaluates hysteresis and linearity deviations to the principle. Inertias and accelerations are combined to give different torque load profiles and the direct and indirect calibration results can join the same "calibration report".

From now on it is necessary to repeat the experiments under different conditions, revalidating the method and analyzing the proposed assembly. Uncertainty of measurement should be part of a parallel discussion.

4. REFERENCES

- [1] DIN 51309 "Werkstoffprüfmaschinen – Kalibrierung von Drehmomentmessgeräten für statische Drehmomente.", DIN (2005).
- [2] C. Bartoli, et al "Dynamic calibration of force, torque and pressure sensors" IMEKO 22nd TC3, 12th TC5 and 3rd TC22 International Conferences (2014).
- [3] J. Schleichert, I. Rahneberg, R. R. Marangoni, T. Fröhlich "Calibration and uncertainty analysis for multicomponent force/torque measurements" Technisches Messen (2016). <https://doi.org/10.1515/teme-2016-0048>

¹CEPEL – Electrical Energy Research Center, Rio de Janeiro, Brazil.

- [4] J. Schleichert, I. Rahneberg, T. Fröhlich, "Calibration of a novel six-degree-of-freedom force/torque measurement system" *Int. J. Mod. Phys. Conf. Ser.* 24 (2013). <http://dx.doi.org/10.1142/S2010194513600173>
- [5] R. S. Oliveira, H. A. Lepikson, T. Fröhlich, R. Theska, W. A. Duboc "A New Proposal for the Dynamic Test of Torque Transducers", XXI Imeko World Congress (2015).
- [6] R. S. Oliveira, H. A. Lepikson, T. Fröhlich, R. Theska, Simon Winter "A new approach to test torque transducers under dynamic reference regimes", *Measurement* (2014) <http://doi.org/10.1016/j.measurement.2014.09.020>
- [7] R. S. Oliveira, *et al* "Estimate of the inertial torque in rotating shafts - a metrological approach to signal processing" *Journal of Physics: Conference Series* (2015). <https://doi.org/10.1088/1742-6596/648/1/012019>
- [8] G. Wegener, T. Bruns, "Traceability of torque transducers under rotating and dynamic operating conditions", *Measurement* (2009).
- [9] L. Klaus, T. Bruns, M. Kobusch, "Determination of Model Parameters for A Dynamic Torque Calibration Device", XX IMEKO World Congress, Busan, Republic of Korea, 2012.
- [10] A. Brüge "Fast Torque Calibrations Using Continuous Procedures" *Imeko TC3 Proceedings* (2002).
- [11] A. Brüge, R. Konya "Investigation on transducers for transfer or reference in continuous torque calibration" *Imeko TC3 Proceedings* (2005).
- [12] S. Nattapon, S. Tassanai "A Comparison of Purely Static and Continuous Torque Calibration Procedure" *IMEKO 22nd TC3, 15th TC5 and 3rd TC22 International Conferences* (2014).